

*More on  
2-D layered materials*

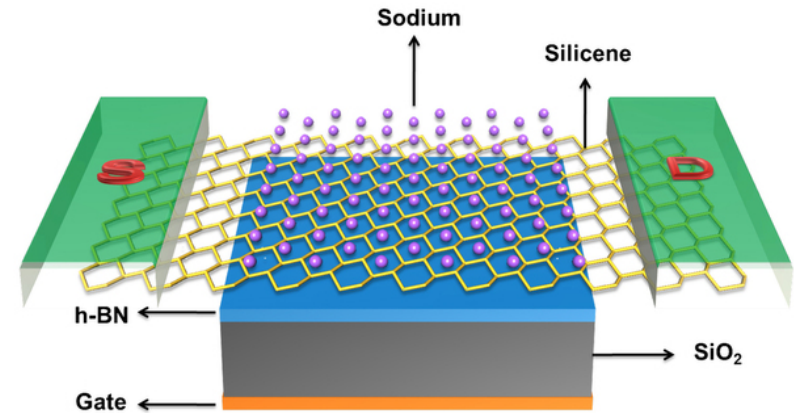
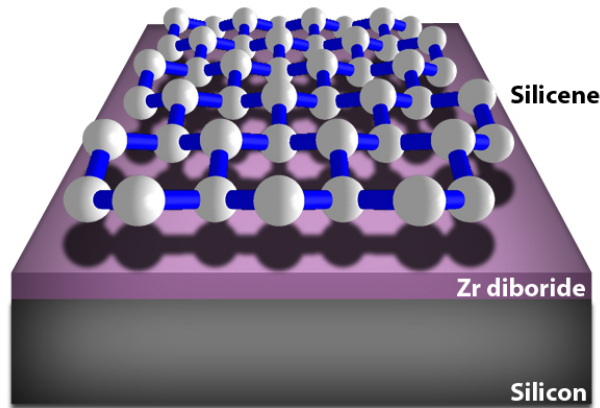
*Graphene-like  
Series*

# *Silicene, Germanene, Stanene, and more....*

- To investigate the growth and characterizations of novel graphene-derived 2D materials, such as *silicene*, *germanene*, *stanene*, *borophene*, *bismuthene*, etc. with the predicted gaps of 2, 24, and 100 meV, respectively for the first three.
- *Stanene* is recently predicted to be quantum spin Hall (QSH) insulator with a large bulk gap  $\sim 0.3$  eV.
- Their QSH states can be effectively tuned by chemical functionalization and external strain, viable for low-power-consumption electronics.

# Another emerging wonder material : Silicene

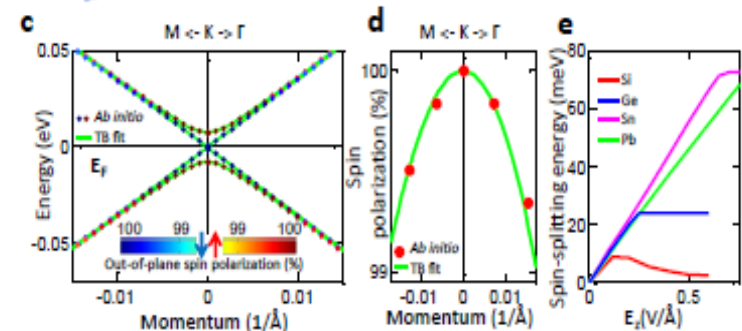
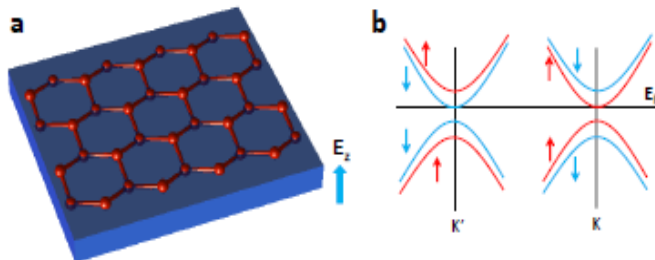
- Graphene-like 2-D silicon
- A finite band gap  $< 0.1\text{V}$ , more compatible with existing silicon-based electronics
- Potential application as a high-performance field effect transistor



*Nature, Scientific Reports 2, 853, 2012*

To grow **Silicene**, **Germanine**, and even **stanene** on insulating or semiconducting substrate.

Superconductivity predicted in alkaline or alkaline earth elements doped silicene ( $\text{CaC}_6$   $T_c = 13\text{K}$ ;  $\text{CaSi}_6$   $T_c = ?$ )

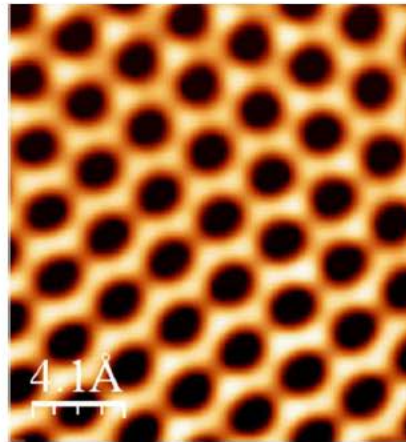


# Silicene

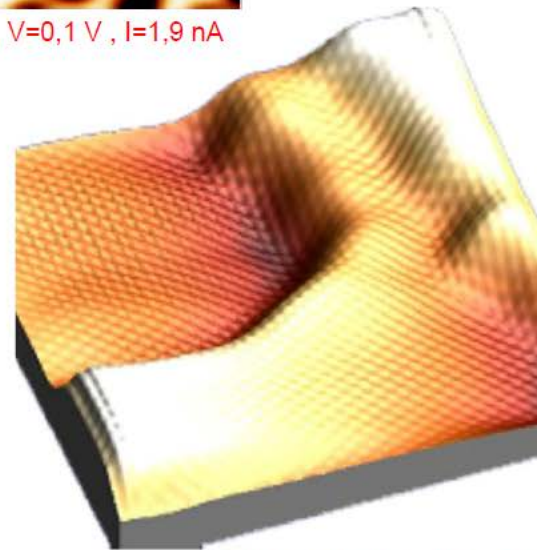
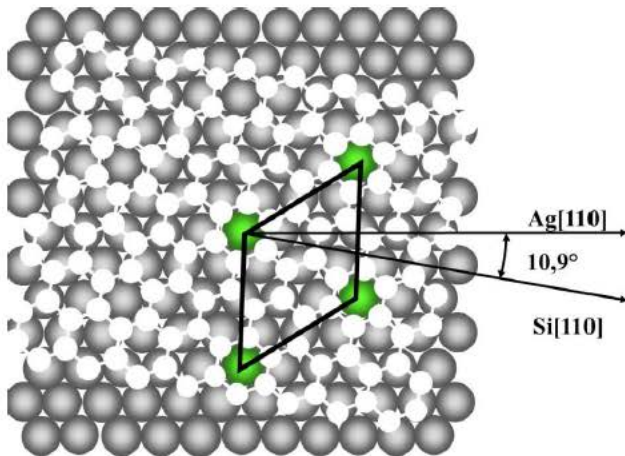
- Via deposition of Si on Ag (111) at 450K -500K.
- B. Lalmi et al, APL (2010), and more.
- A **buckled** structure with a small gap of  $\sim 1.5$  mV

Si/Ag(111)

$(2\sqrt{3} \times 2\sqrt{3})R30^\circ$



22x22 nm<sup>2</sup> , V=0,1 V , I=1,9 nA



B. Lalmi et al, APL, 97, 223109 (2010)

Electronic properties (HRPES)

(4x4) superstructure

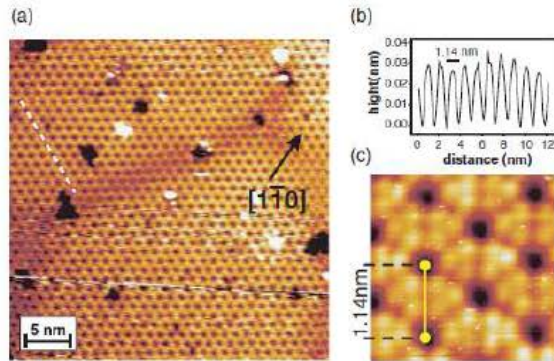


FIG. 2 (color). (a) Filled-states STM image of the 2D Si layer on Ag(111)-(1 × 1) ( $U_{\text{bias}} = -1.3$  V,  $I = 0.35$  nA). Clearly visible is the honeycomblike structure. (b) Line profile along the dashed white line indicated in (a). The dark centers in the STM micrograph are separated by 1.14 nm, corresponding to  $\sqrt{3}$  times the Ag(111) lattice constant, in agreement with the  $(4 \times 4)$  symmetry. (c) High-resolution STM topograph ( $3 \times 3$  nm,  $U_{\text{bias}} = -1.3$  V,  $I = 0.35$  nA) of the Si adlayer.

Dirac cone

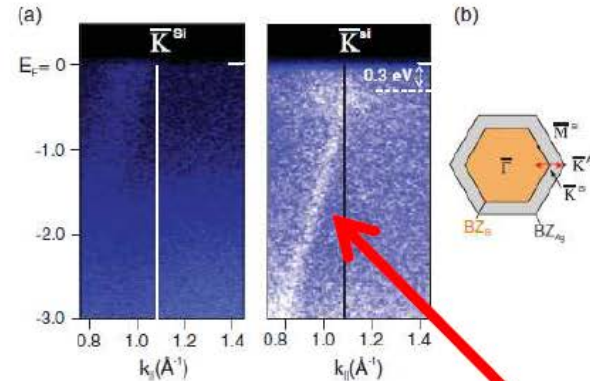


FIG. 3 (color). (a) ARPES intensity map for the clean Ag surface (left) and after formation of the 2D Si adlayer (right), taken along the Ag  $\bar{\Gamma}$ - $\bar{K}$  direction through the silicene  $\bar{K}$  ( $h\nu = 126$  eV). (b) Brillouin-zone (BZ) scheme of the 2D Si layer with respect to the Ag(111)-(1 × 1) surface. The red arrow indicates the ARPES measurement direction.

Linear dispersion

PHYSICAL REVIEW B 87, 245430 (2013)

## Absence of a Dirac cone in silicene on Ag(111): First-principles density functional calculations with a modified effective band structure technique

Yun-Peng Wang and Hai-Ping Cheng\*

*Quantum Theory Project and Department of Physics, University of Florida, Gainesville, Florida 32611, USA*

(Received 22 February 2013; revised manuscript received 3 April 2013; published 24 June 2013)

We investigate the currently debated issue of the existence of the Dirac cone in silicene on an Ag(111) surface, using first-principles calculations based on density functional theory to obtain the band structure. By unfolding the band structure in the Brillouin zone of a supercell to that of a primitive cell, followed by projecting onto Ag and silicene subsystems, we demonstrate that the Dirac cone in silicene on Ag(111) is destroyed. Our results clearly indicate that the linear dispersions observed in both angular-resolved photoemission spectroscopy [P. Vogt *et al.*, *Phys. Rev. Lett.* **108**, 155501 (2012)] and scanning tunneling spectroscopy [L. Chen *et al.*, *Phys. Rev. Lett.* **109**, 066804 (2012)] come from the Ag substrate and not from silicene.

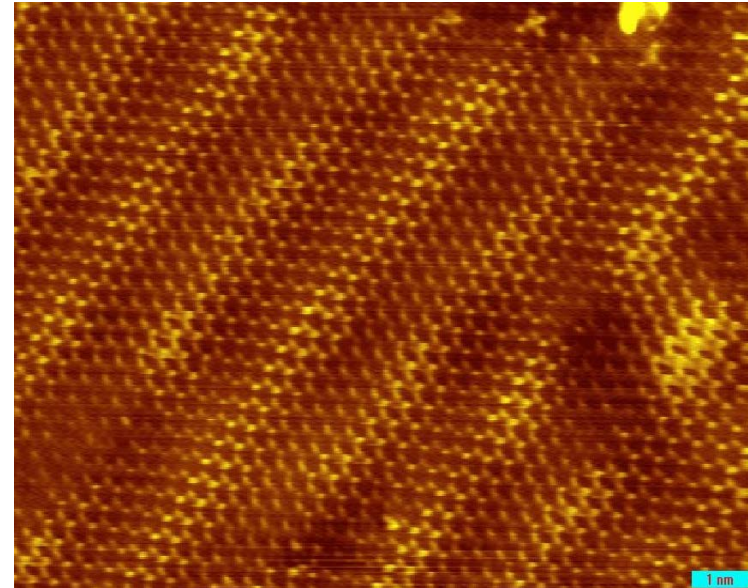
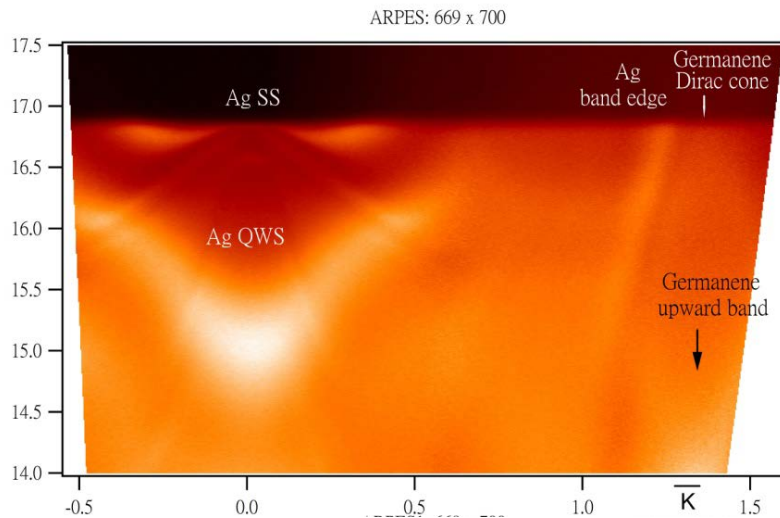
No Dirac cone

???

Y-P. Wang et al *Phys. Rev. B.* 87 245430 (2013)

# Demonstration of Germanene:

## Germanene grown on Ag (111)



**First observation of Dirac cone**

**First observation of “real” honeycomb**

Prof. Shu-jung Tang et al, NTHU, (2015)  
Phys. Rev. Materials **2**, 024003, (2018)

- To grow silicene on 2D-MoS<sub>2</sub> ?
- To grow Germanene on 2D-MoS<sub>2</sub> ?

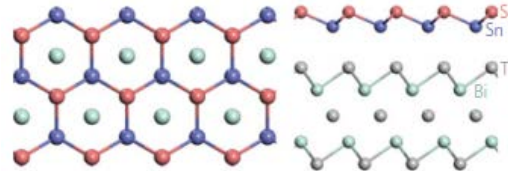
**YES!**

However, it is metallic!

L. Zhang et al., Phys. Rev. Lett. 116, 256804 (2016)

# Stanene

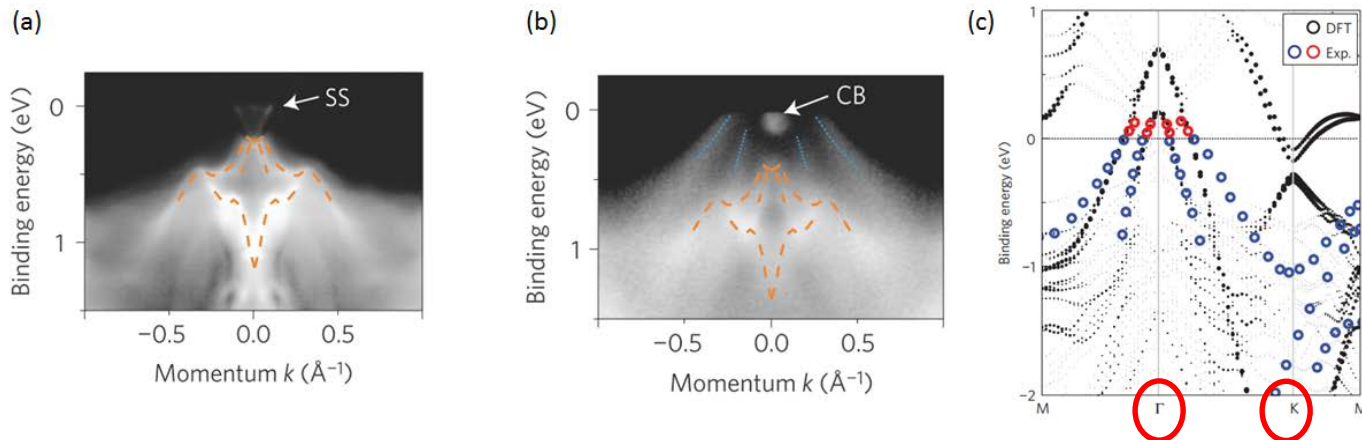
- Tin ( $Sn$ ) with its large spin-orbit coupling offers rich electronic structures
- Predicted to exhibit highly efficient thermoelectrics, topological superconductivity, high-temperature quantum spin Hall, and quantum anomalous Hall effects.
- *Stanene could support a large gap ( $\sim 0.3$  V) 2-D quantum spin Hall (QSH) state, thus enable the dissipationless electric conduction at RT.* Y. Xu et al. *PRL* **111**, 136804 (2013).
- Integrability with conventional semiconductor industry.
  - ✓ With its elemental nature,  $Sn$  is free from the stoichiometry and related defects.
  - ✓  $Sn$  is commonly used in many group-IV MBE system and is easy to tackle.
- In this 2-D materials, outstanding properties: The Fermi velocity near Dirac point approaches  $7.3 \times 10^5$  m/s, much larger than that of typical 3-D TI, and close to that of graphene ( $1 \times 10^6$  m/s).
- stanene/ $Bi_2Te_3$ (111) crystal structure
- $\alpha$ - $Sn$  (001) film was grown on  $InSb$ (001) as a 3-D TI, with nearly massless electron dispersion with a bulk bandgap of 230 mV, showing spin helical band by ARPES.
- One monolayer (111) orientated  $\alpha$ - $Sn$  is a buckled-honeycomb structure, similar to graphene.



F. Zhu et al.  
*Nature Materials*, **14**,  
1020–1025 (2015).

# Stanene grown on $\text{Bi}_2\text{Te}_3(111)$

- Monolayer stanene was fabricated by MBE on  $\text{Bi}_2\text{Te}_3(111)$  substrate.
- **Obvious discrepancies** :
  - According to ARPES, the valence bands of stanene are pinned in the conduction band of  $\text{Bi}_2\text{Te}_3(111)$ , giving metallic interface states. **The inverted bandgap at  $\Gamma$  point, the key to QSH state, was not observed.**
  - Dirac-cone-like features at K point are expected in a honeycomb structure, stanene with a larger SOC, leads to a bandgap of **0.1 eV** at the Dirac-cone. **However, Dirac-cone at the K-point of stanene / $\text{Bi}_2\text{Te}_3(111)$  was not observed.**



F. Zhu *et al.*  
*Nature Materials*, **14**,  
1020–1025 (2015).

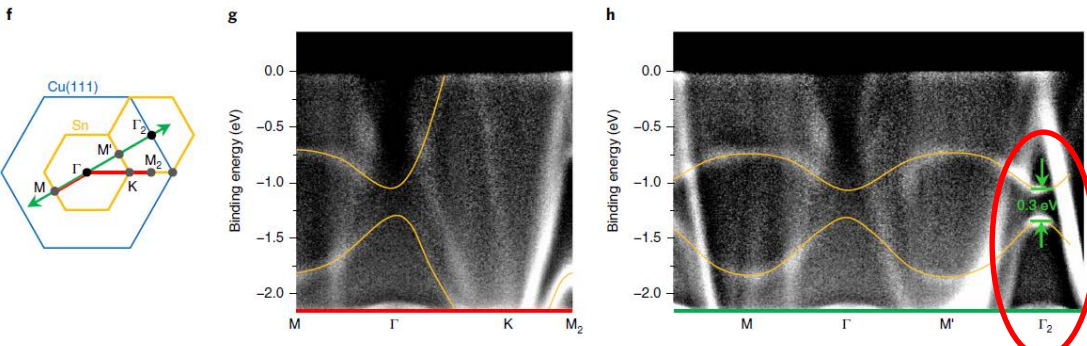
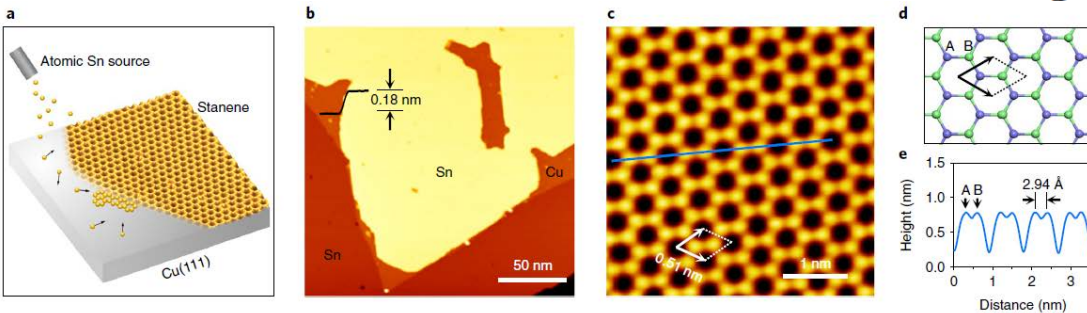
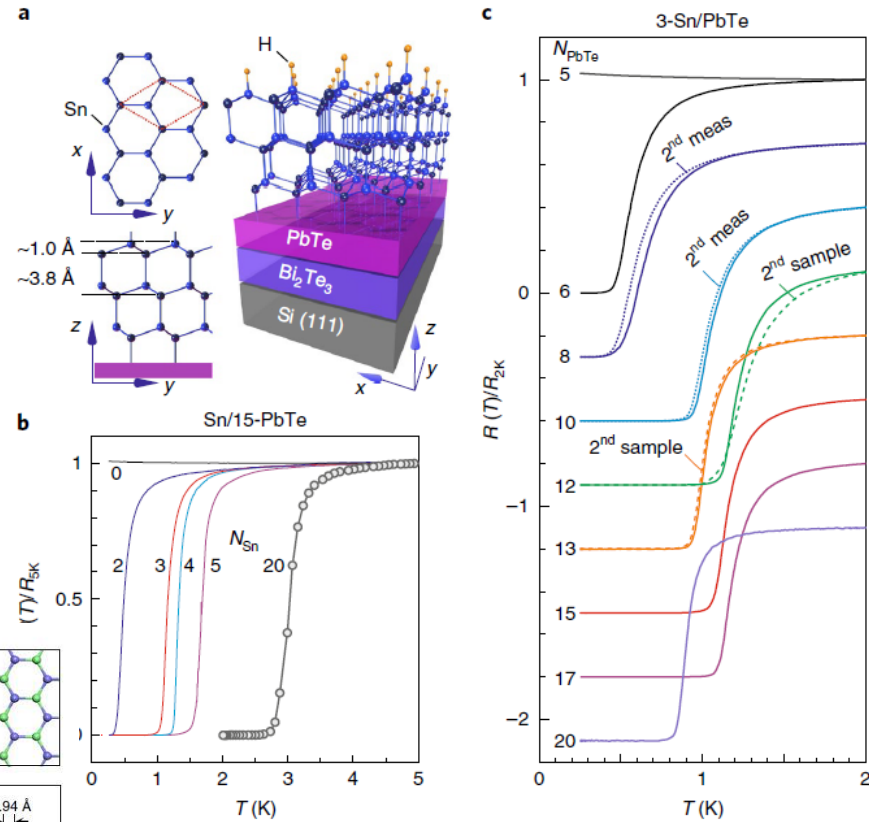
(a) ARPES spectra of  $\text{Bi}_2\text{Te}_3(111)$ , (b) stanene on  $\text{Bi}_2\text{Te}_3$  along K- $\Gamma$ -K direction. The orange dashed lines mark the bulk band dispersions of  $\text{Bi}_2\text{Te}_3$ . The blue dotted lines mark the hole band of stanene. SS marks the surface state and CB marks the conduction band of  $\text{Bi}_2\text{Te}_3$ . (c) Comparison of experimental results with DFT calculation of stanene/ $\text{Bi}_2\text{Te}_3$ . Red dots above the Fermi level are obtained by *in-situ* potassium deposition that provides the film with electrons.

# Progress on Stanene

- Discover superconductivity in few-layer stanene down to a bilayer grown on PbTe, while bulk  $\alpha$ -tin is not superconductive.

a trilayer stanene on top of PbTe/Bi<sub>2</sub>Te<sub>3</sub>/Si(111)

- Stanene on Cu(111) by low-T MBE. Discovered an unusually flat stanene showing an *in-plane* *s-p* band inversion with a SOC-induced topological gap ( $\sim 0.3$  eV) at the  $\Gamma$  point, which represents a group-IV graphene-like material displaying topological features.



Nature Physics, 14, 344, (2018).

Nature Materials, 17, 1081, (2018).

# Borophene

The  $\beta_{12}$  sheet, a borophene structure that can form spontaneously on a Ag(111) surface.

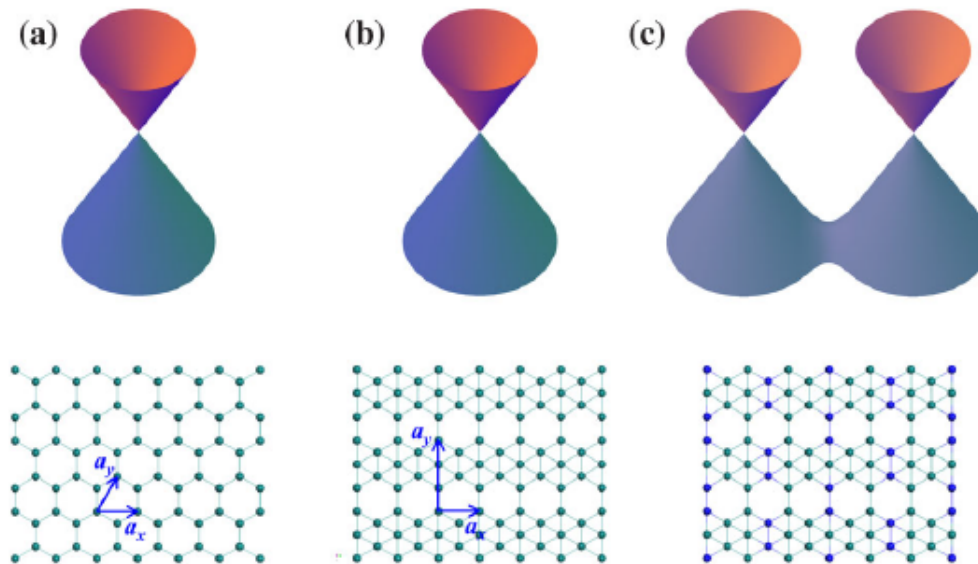
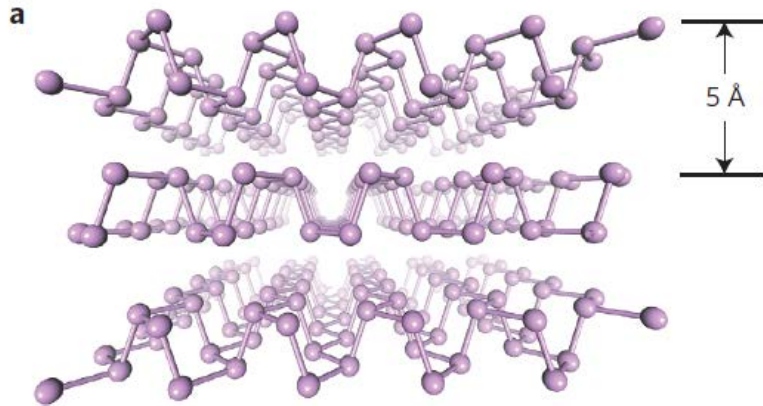


FIG. 1. Schematic drawing of the Dirac cones and lattices. (a) Honeycomb structure. (b)  $\beta_{12}$  sheet. (c) The  $\beta_{12}$  sheet with a  $3 \times 1$  perturbation. The blue and green balls indicate the boron atoms with different on-site energies in our TB analysis. The top and bottom panels are the band structures and atomic structures, respectively. The basic vectors of the primitive unit cell are indicated by the blue arrows.

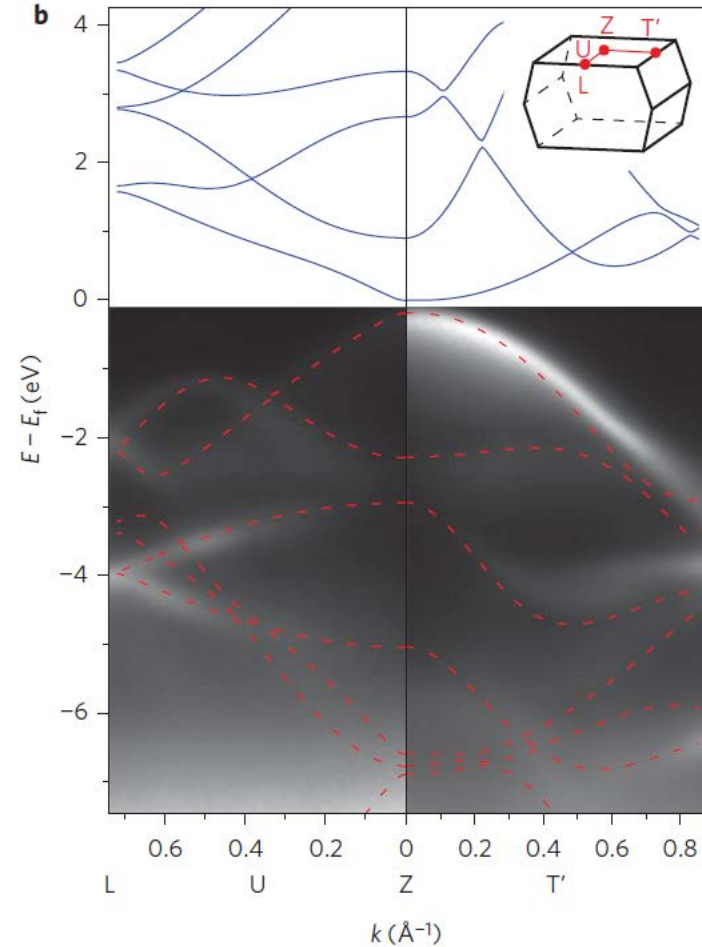
# Phosphorene

- Black phosphorus, *phosphorene* is one of three different crystal structures that pure phosphorus can adopt.
- White phosphorus is used in making fireworks.
- Red phosphorus is used to make the heads of matches.
- The bandgap is adjusted by varying the number of phosphorene layers stacking one atop another, significantly larger than the bulk value of 0.31- 0.36 eV.
- Much easier to engineer devices with the exact behavior desired.
- **Mobility ~ 600**
- Unstable in air.
- Passivated by Al<sub>2</sub>O<sub>3</sub> layer and teflon.
- Harnessing phosphorene's higher electron mobility for making electronic devices.

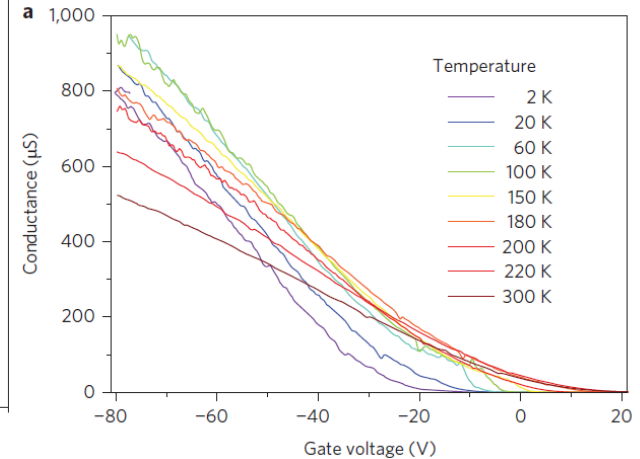
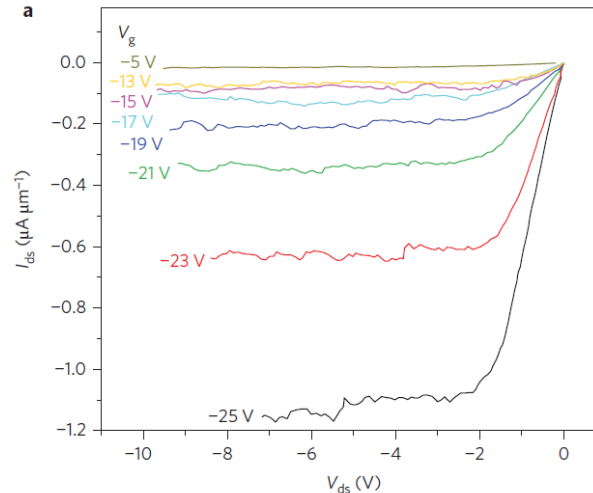
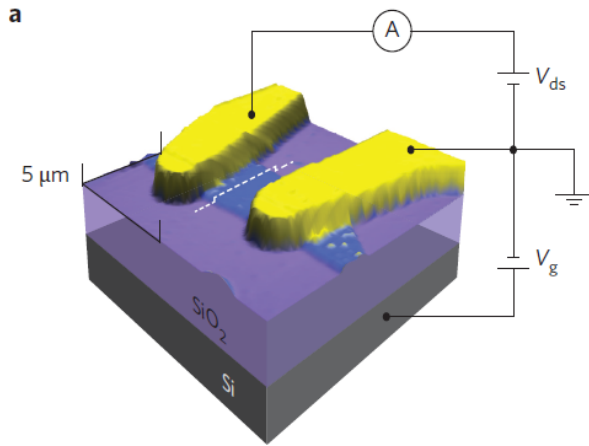
# Phosphorene



- Black phosphorus was synthesized under a constant pressure of 10 kbar by heating red phosphorus to 1,000 C .
- Then slowly cooling to 600 C at a cooling rate of 100 C per hour.

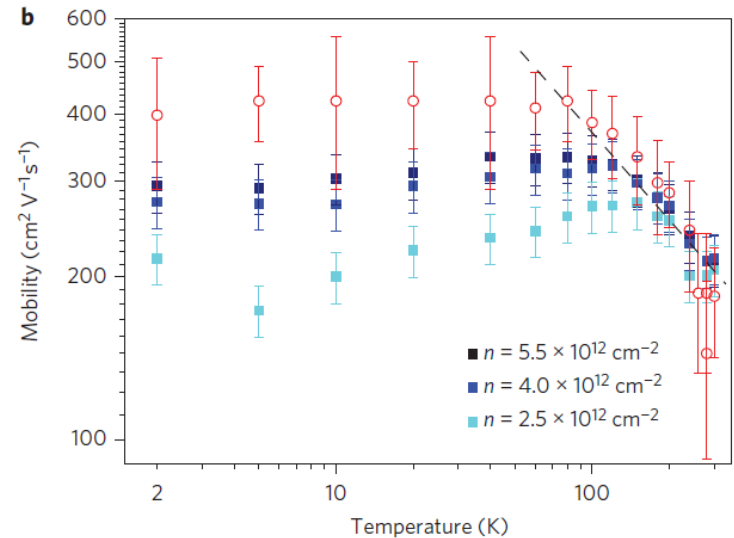


# Phosphorene



- Reliable transistor performance is achieved at room temperature in samples thinner than 7.5 nm. Channel length and width of the device are 1.6 mm and 4.8mm.
- Field-effect mobility** (red open circles), and **Hall mobility** (filled squares, three different values of  $n$ ) as a function of temperature on a logarithmic scale

$$\mu_{FE} = \frac{L}{W} \frac{1}{C_g} \frac{dG}{d(V_g - V_{th})} \quad \mu_H = \frac{L}{W} \frac{G}{ne}$$



# Phosphorene

- fabricating *p*-type FETs based on few-layer phosphorene.
- exhibit ambipolar behavior with drain current modulation up to  $10^5$ .
- a field-effect mobility to  $\sim 600$  cm<sup>2</sup> V<sup>-1</sup> s<sup>-1</sup> at room temperature, and thickness dependent.

Tomanek at Michigan State, and Peter Ye at Purdue reported phosphorene-based transistors, along with simple circuits. ACS Nano, 8 (4), 4033–4041, (2014).

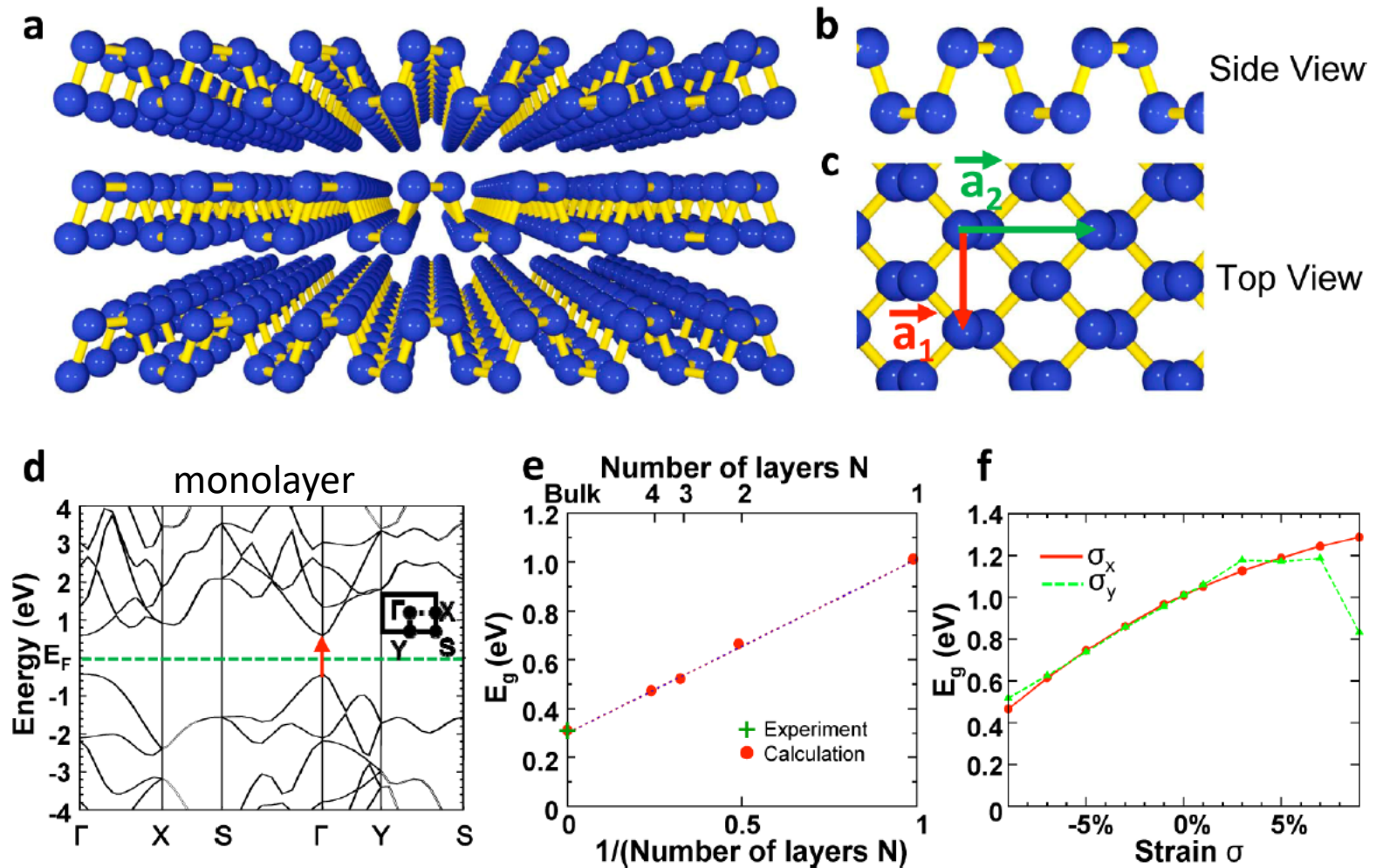
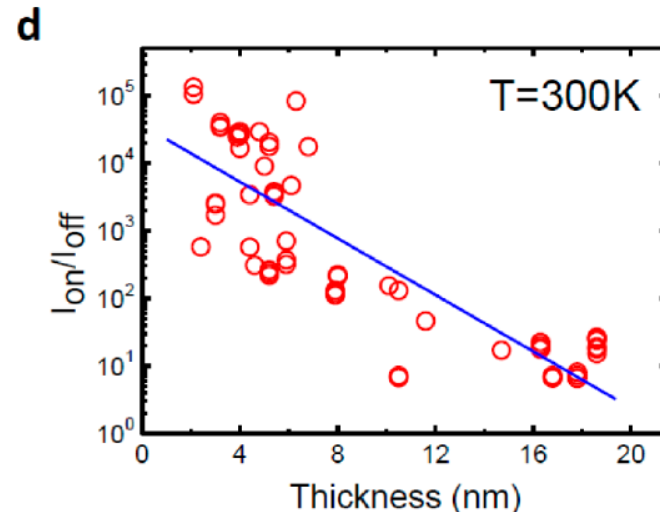
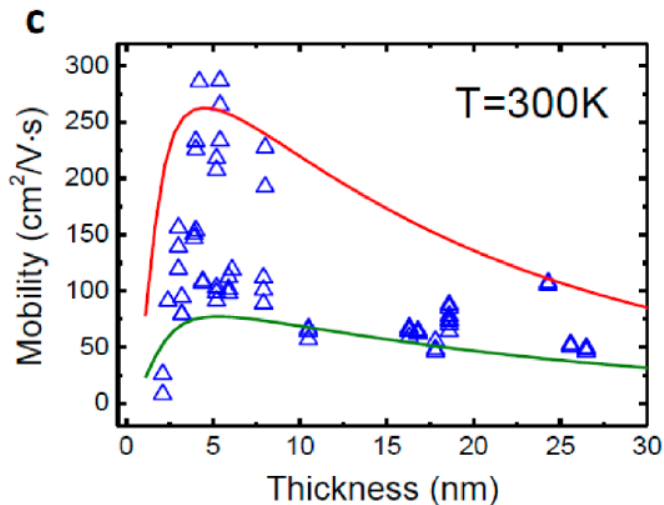
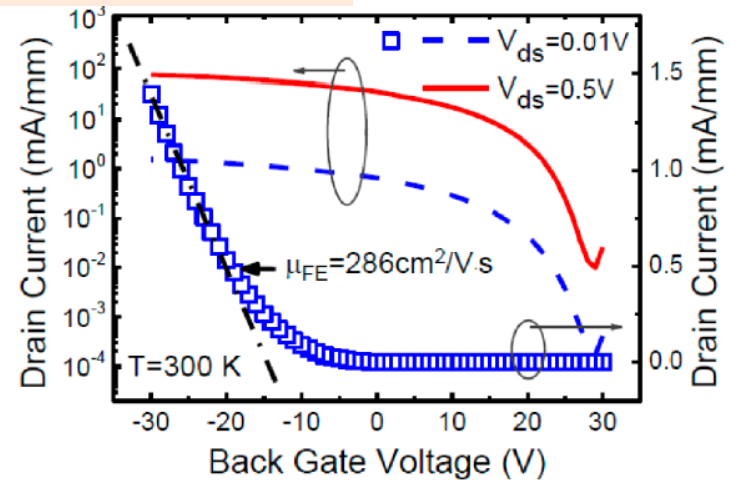
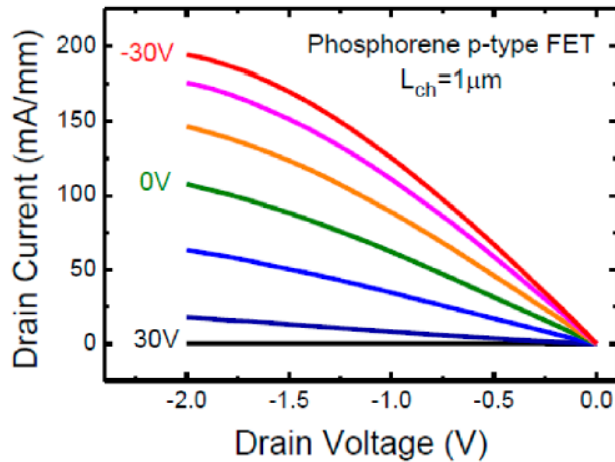


Figure 1. Crystal structure and band structure of few-layer phosphorene. (a) Perspective side view of few-layer phosphorene. (b,c) Side and top views of few-layer phosphorene. (d) DFT-HSE06 band structure of a phosphorene monolayer. (e,f) DFT-HSE06 results for the dependence of the energy gap in few-layer phosphorene on (e) the number of layers and (f) the strain along the x- and y-direction within a monolayer. The observed band gap value in the bulk is marked by a cross in (e).

## Phosphorene-based field effect transistors



- Tomanek and Ye reported to have made phosphorene-based transistors, along with simple circuits. [ACS Nano, 8 \(4\), 4033–4041, \(2014\).](#)
- A few-layer phosphorene FET with  $1.0\ \mu\text{m}$  channel length displays (a, b) high on-current of **194 mA/mm**, (c) high hole field-effect mobility of  **$286\ \text{cm}^2\text{V}^{-1}\cdot\text{s}^{-1}$** , (d) an on/off ratio of  **$10^4$** .
- Constructed a **CMOS inverter** by a phosphorene  $p$ -MOS transistor and a  $\text{MoS}_2$   $n$ -MOS transistor.

# Bismuthene

- Quantum spin Hall materials with dissipationless spin currents required cryogenic temperatures owing to small energy gaps.
- A room-temperature regime with a large energy gap may be achievable that exploits the atomic spin-orbit coupling (SOC).
- The concept is based on a substrate-supported monolayer of a **high-atomic number element**, and is realized as a **bismuth honeycomb lattice** on top of the insulating substrate SiC(0001). Using STS, a gap of  $\sim 0.8$  eV and conductive edge states are detected, consistent with theory.

Reis et al., Science **357**, 287–290 (2017)

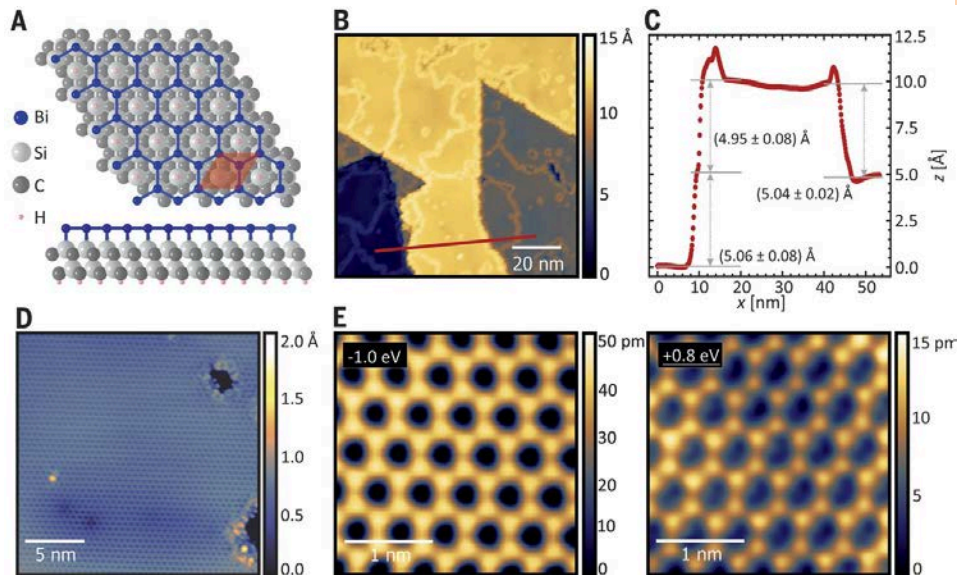
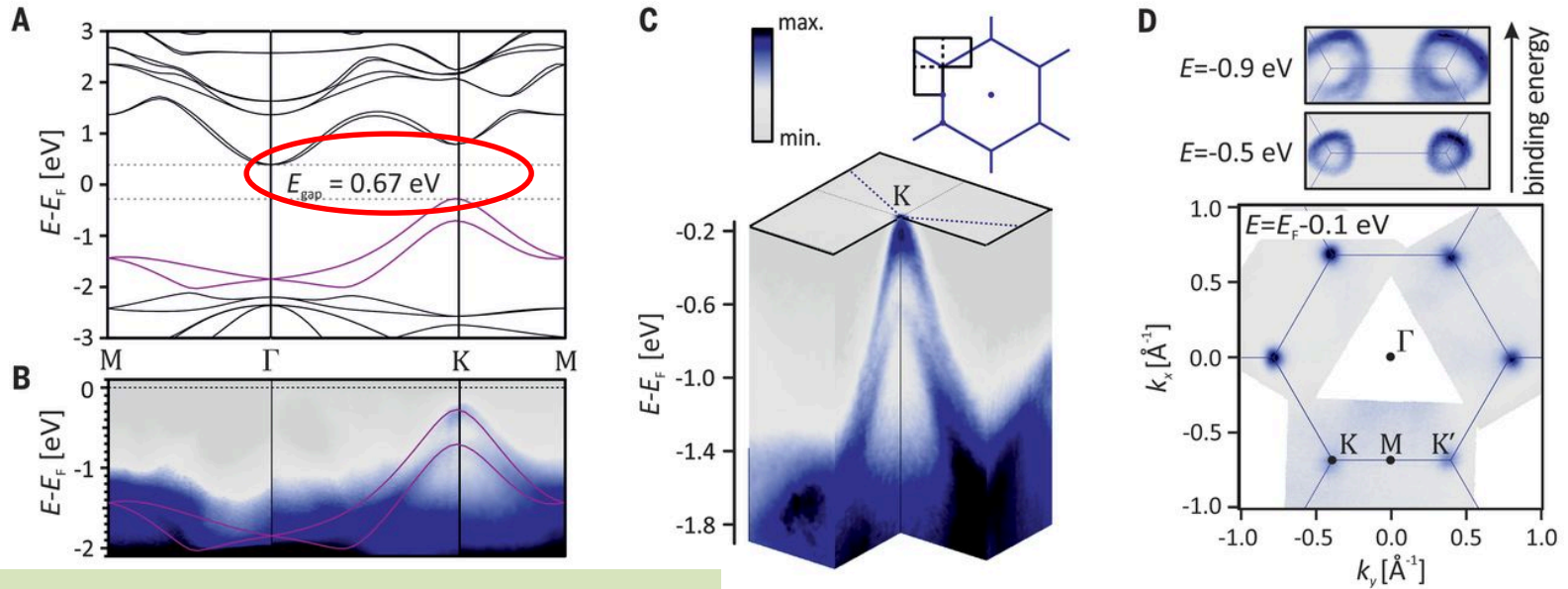
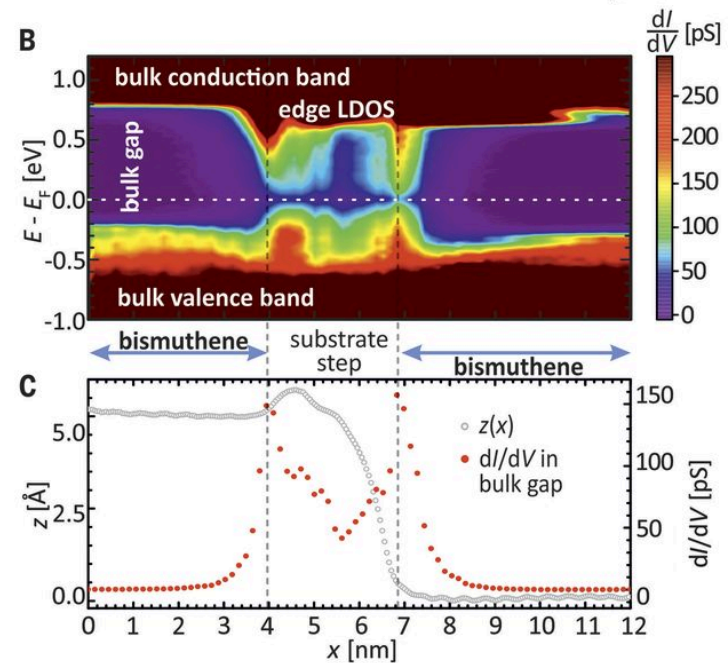
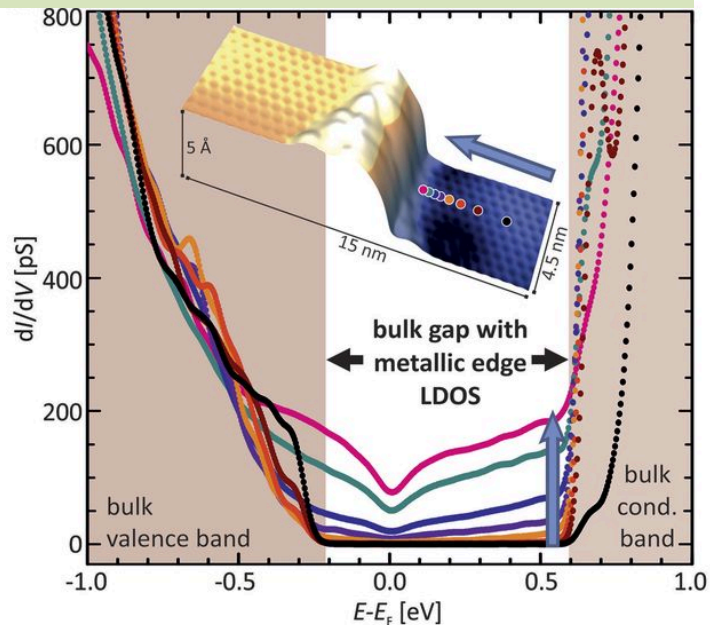


Fig. 1 **Bismuthene on SiC(0001) structural model.** (A) Sketch of a bismuthene layer placed on the threefold-symmetric SiC(0001) substrate in Embedded Image commensurate registry. (B) Topographic STM overview map showing that bismuthene fully covers the substrate. The flakes are of  $\sim 25$ -nm extent, limited by domain boundaries. (C) Substrate step-height profile, taken along the red line in (B). The step heights correspond to **SiC steps**. (D) The honeycomb pattern is seen on smaller scan frames. (E) Close-up STM images for occupied and empty states (left and right panels, respectively). They confirm the formation of **Bi honeycombs**.

# Bismuthene



## Bismuthene over a SiC step of 5Å height



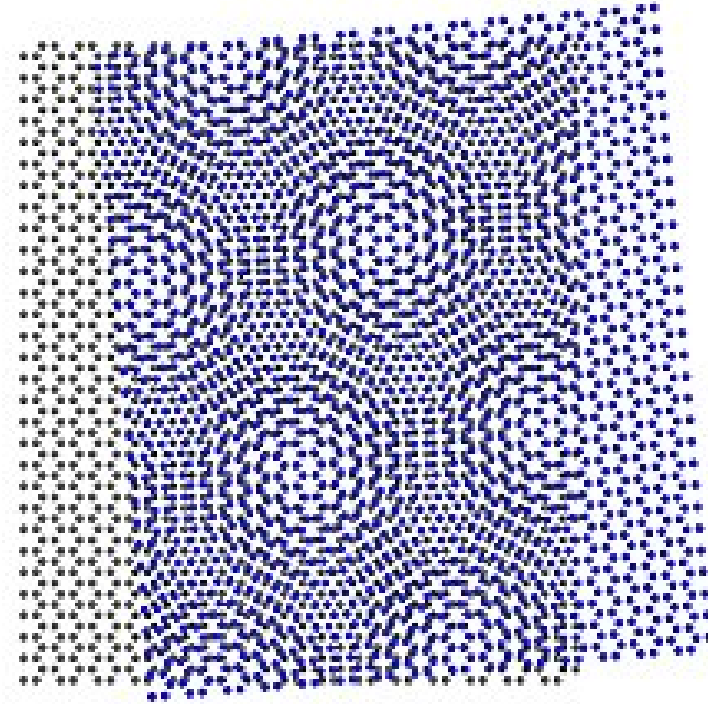
Twisted Graphene

Twistronics

# Twisted graphene

- The behavior of **strongly correlated** materials, and in particular unconventional superconductors, has been studied for decades, but is still not well understood.
- Prof. Pablo Jarillo-Herrero and his student Yuan Cao of MIT discovered in 2018 that superconductivity existed in twisted bilayer graphene. For twist angles of about  $1.1^\circ$ —forming a Moire pattern at 1.7K, the electronic band structure of **this ‘twisted bilayer graphene’ exhibits flat bands near zero Fermi energy, resulting in correlated insulating states at half-filling.**
- Upon electrostatic **doping** of the material away from these correlated insulating states, they observed **tunable** zero-resistance states with a  $T_c$  up to **1.7K**.
- Twisted bilayer graphene is thus a precisely tunable, purely carbon-based, 2-D superconductor. **It is therefore an ideal material for investigations of strongly correlated phenomena.**
- They also found the addition of BN between the two graphene layers, **orbital magnetism** was produced at the magic angle of  $1.17^\circ$ . Spectroscopic study showed strong electron–electron correlation at this magic angle.

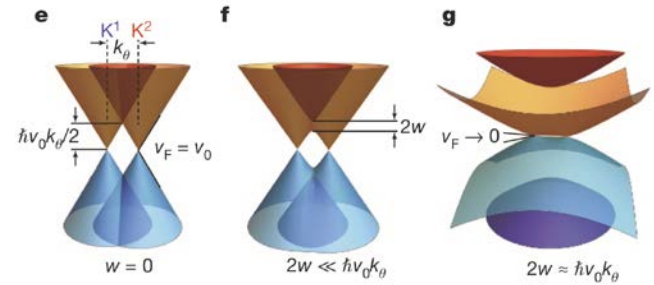
Moire Pattern



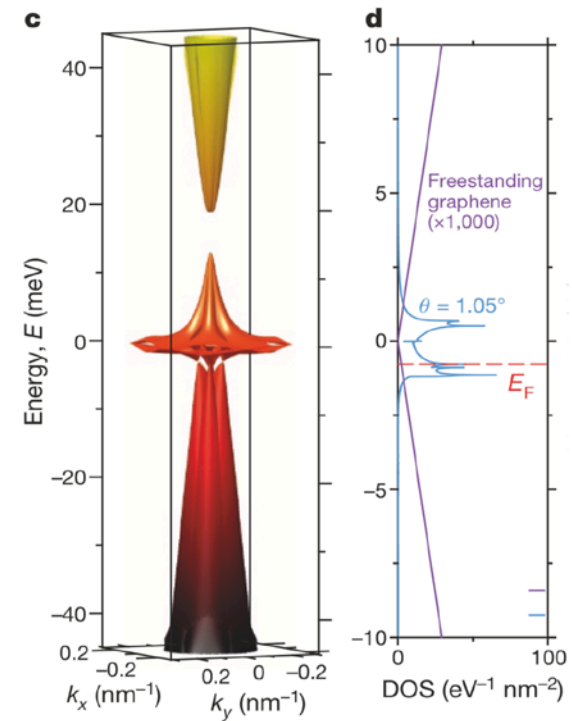
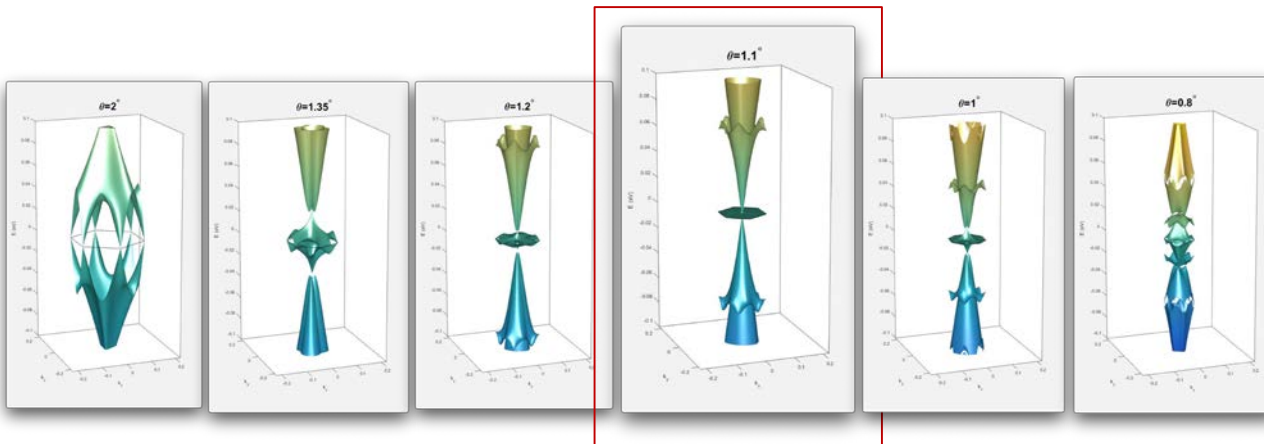
Yuan Cao et al,  
Nature **556**, 43–50 (2018).  
Nature **556**, 80–84 (2018).

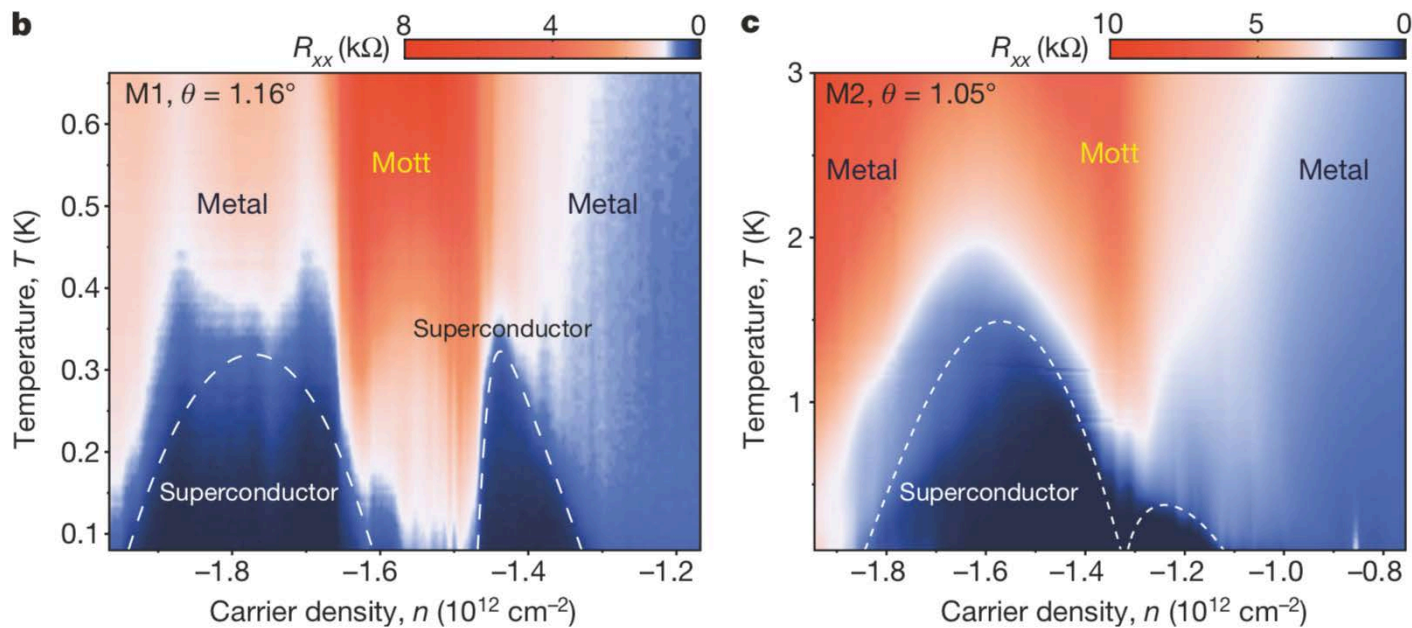
# Emergence of flat band in TBG

- **Hybridization between adjacent Dirac cones** reduces the Fermi velocity at the charge neutrality point. (typical value:  $\sim 10^6 \text{ ms}^{-1}$ )
- At low twist angles, each electronic band in the mini Brillouin zone has a **four-fold degeneracy of spins and valleys**, the latter inherited from the original electronic structure of graphene
- **Reduction of the Fermi velocity and the increase of localization**
- No any appreciable superconductivity when the fermi energy was tuned into the flat conduction bands ( $E_F > 0$ ).
- **Magic angle (flat band):  $1.1^\circ$**



Cao, Y. et al., *Nature* 556, 26154 (2018).





- Domes corresponding to superconducting states.

Four-probe resistance  $R_{xx}$  measured. Two superconducting (SC) domes are clearly observed next to the half-filling state ("Mott", centered around  $-ns/2 = -1.58 \times 10^{12}$  cm $^{-2}$ ). The remaining regions in the diagram are labeled as "Metal" due to the metallic temperature dependence. The highest critical temperature observed in device M1 is  $T_c = 0.5$  K (50% normal state resistance). (c) Similar plot as in (b) but measured in device M2, showing two asymmetric and overlapping domes. The highest critical temperature in this device is  $T_c = 1.7$  K.

# Promising works

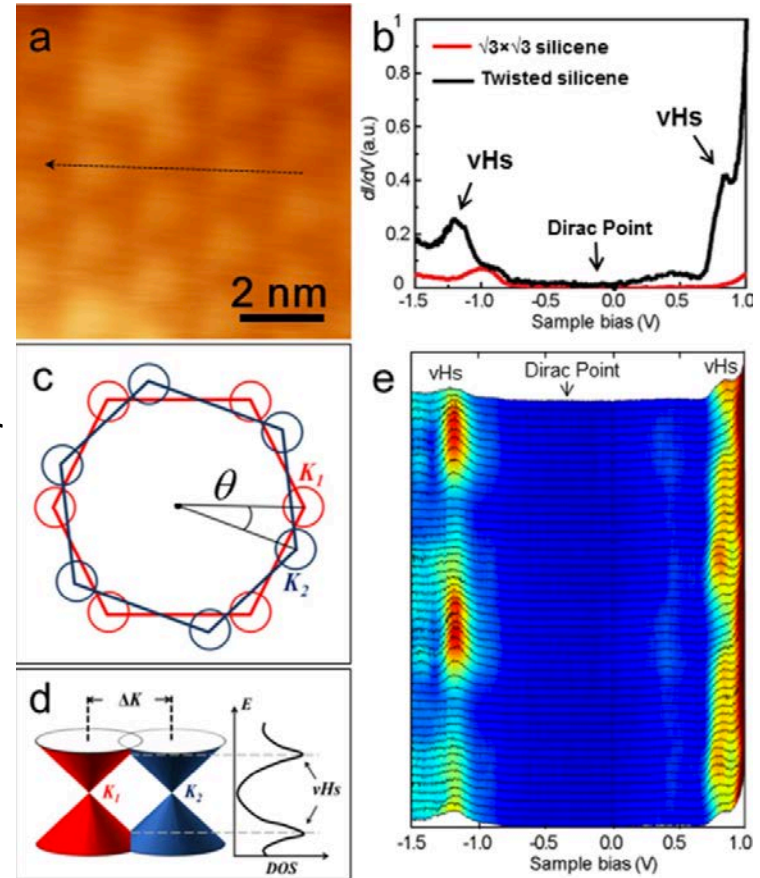
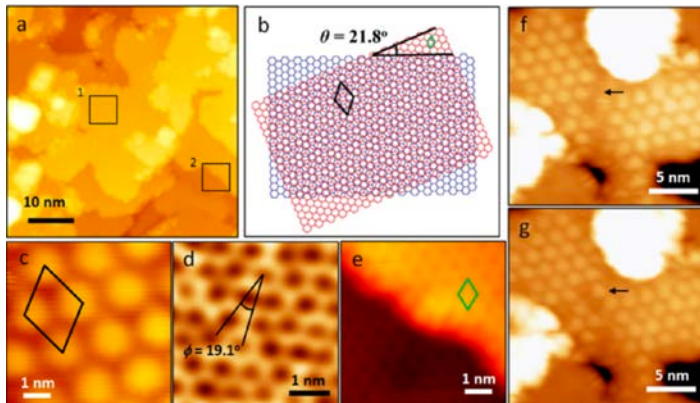
- (1) Adjusting **twist angle** and applying **perpendicular electric fields** by means of differential gating → fine-tuned the **interactions** of two graphene layers
- (2) Applying **pressure** to the graphene superlattice to increase the interlayer hybridization and **Coupling** different magic-angle TBG structures to induce **Josephson coupling** in the vertical direction → **enhance Tc**
- (3) **ARPES measurements** → directly probe the band structure for more detailed information.

However, the work might be hard to achieve due to difficulties such as removing the top h-BN layer.

- (4) The **magic-angle superlattices** and **flat-band electronic structures** could also be realized with other two-dimensional materials or lattices to investigate strongly correlated systems with different properties.

# Twisted Silicene Multilayers

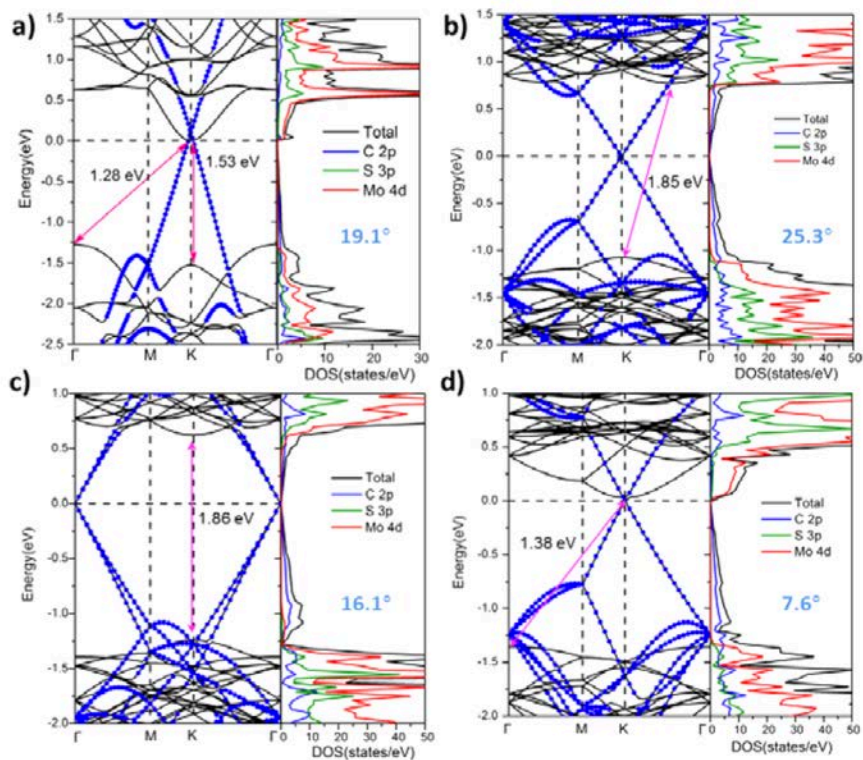
- **Buckled-structure**
- Peaks: interlayer-rotation-induced **Van Hove singularity (VHS)** in the DOS.
- **21.8°** is the largest rotation angle between two honeycomb lattices that can produce a commensurate superlattice.
- The silicon  $sp_2$ - $sp_3$  mixed hybridization states lead to a robust interlayer interaction in multilayer silicene, which is much stronger than the interlayer interaction in graphene.
- It paves the way for developing ultrathin optical devices



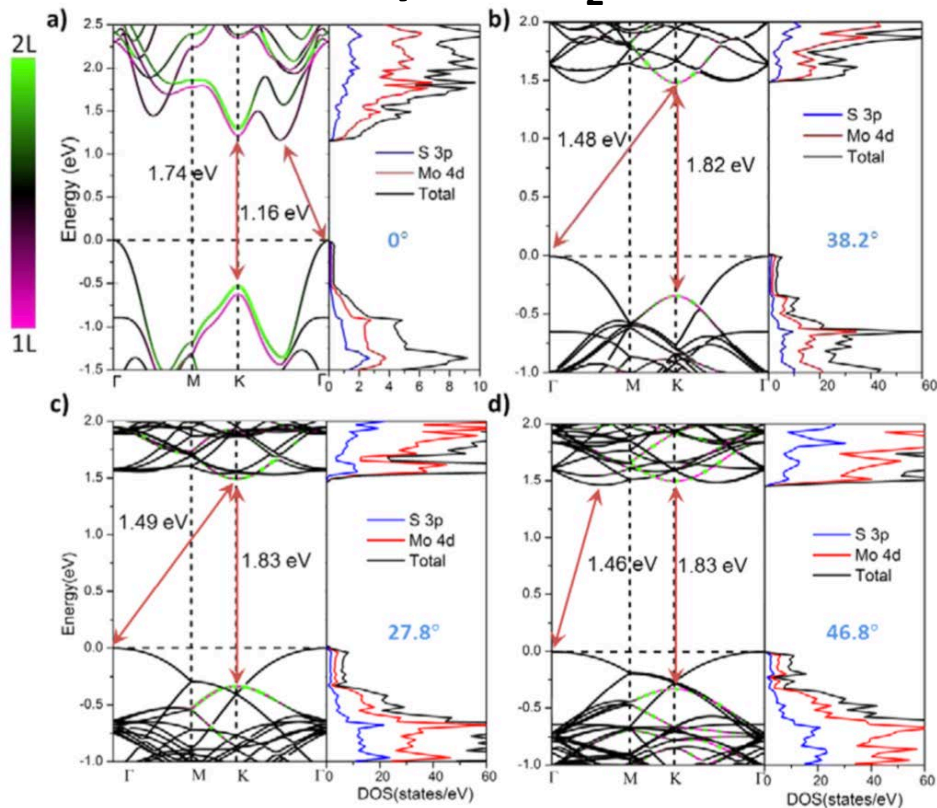
Zhi Li et al., ACS Cent. Sci. 2, 517–521 (2016)

# Theoretical Predictions

## Twisted Graphene/MoS<sub>2</sub>

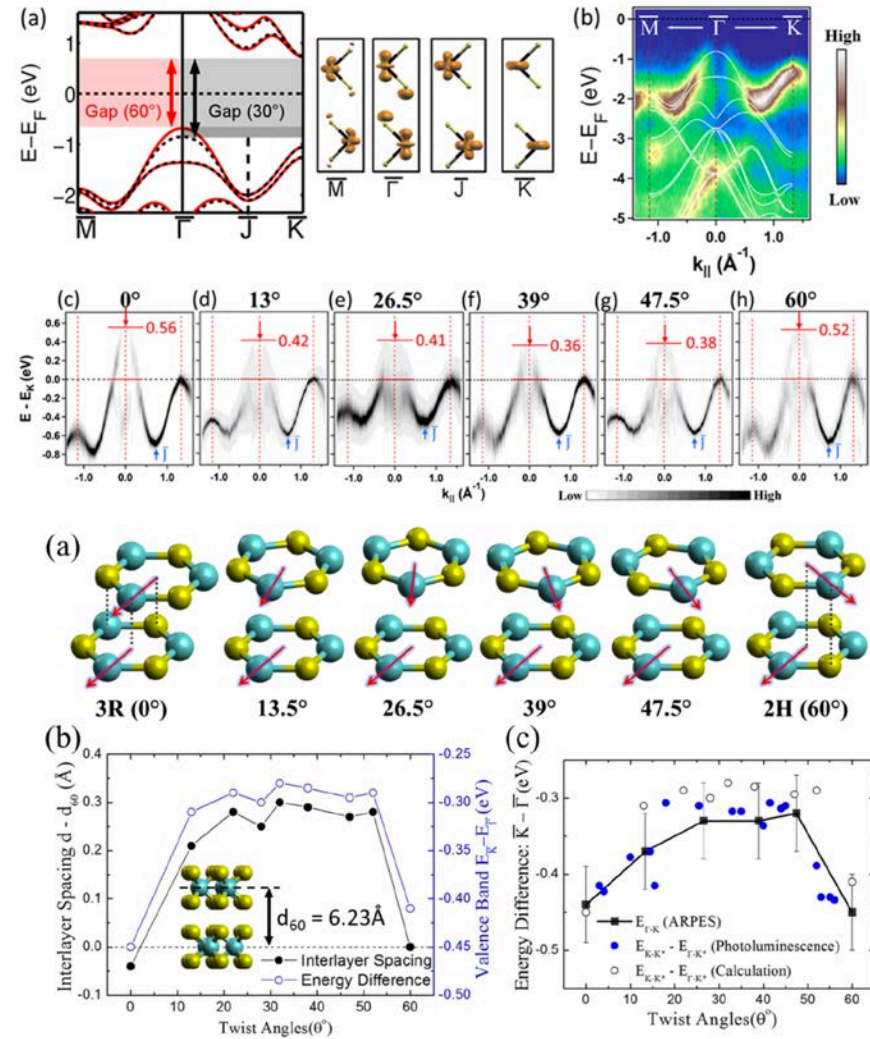


## Twisted Bilayer MoS<sub>2</sub>



# Twisted Bilayer MoS<sub>2</sub>

- One of the well-known consequences of interlayer coupling in TMDs is the direct-to-indirect bandgap transition from monolayer to multilayer films.
- The valence band maxima (VBM) lies at  $\Gamma$  instead of  $\bar{K}$ , contrary to ML MoS<sub>2</sub> → **indirect transition**.
- Increasing the twist angle of TB-MoS<sub>2</sub> from 0° to 30–40° leads to an increase in the **interlayer spacing**, and thus a decrease in the **interlayer coupling**  
 → **downward shift of VBM**
- **A twist-angle independent exciton binding energy** → controlling the change in the bandgap in a bilayer MoS<sub>2</sub> system by interlayer twist angle



# Twisted Graphene/MoS<sub>2</sub>

- The electronic structure of mono-layer graphene is essentially intrinsic when it is an overlayer on MoS<sub>2</sub> regardless of the twist angle.

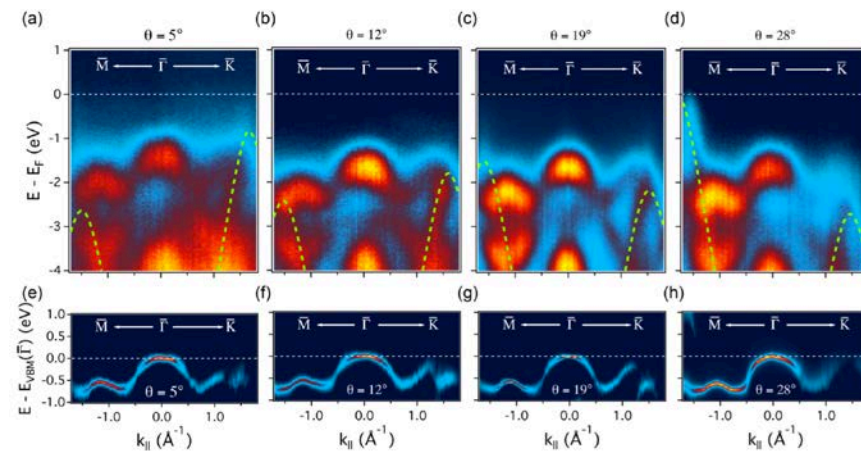
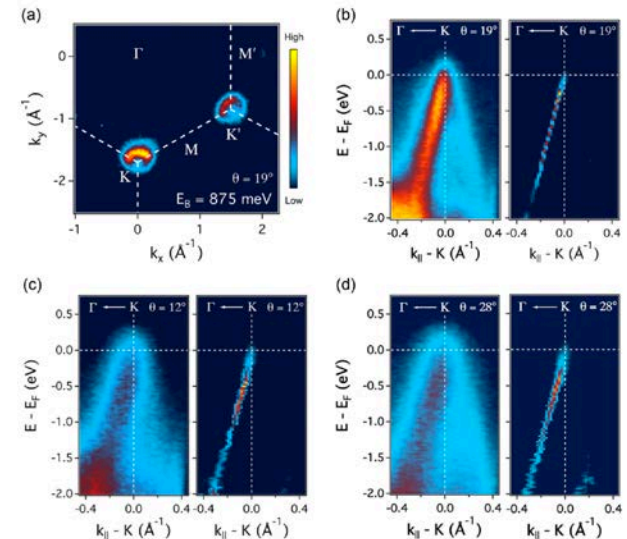
→ monolayer MoS<sub>2</sub> is an ideal substrate for preserving the **intrinsic properties of monolayer graphene**.

- Gr-derived bands are very close to intrinsic and that the Gr-derived Dirac point is situated **within the MoS<sub>2</sub> band gap**.

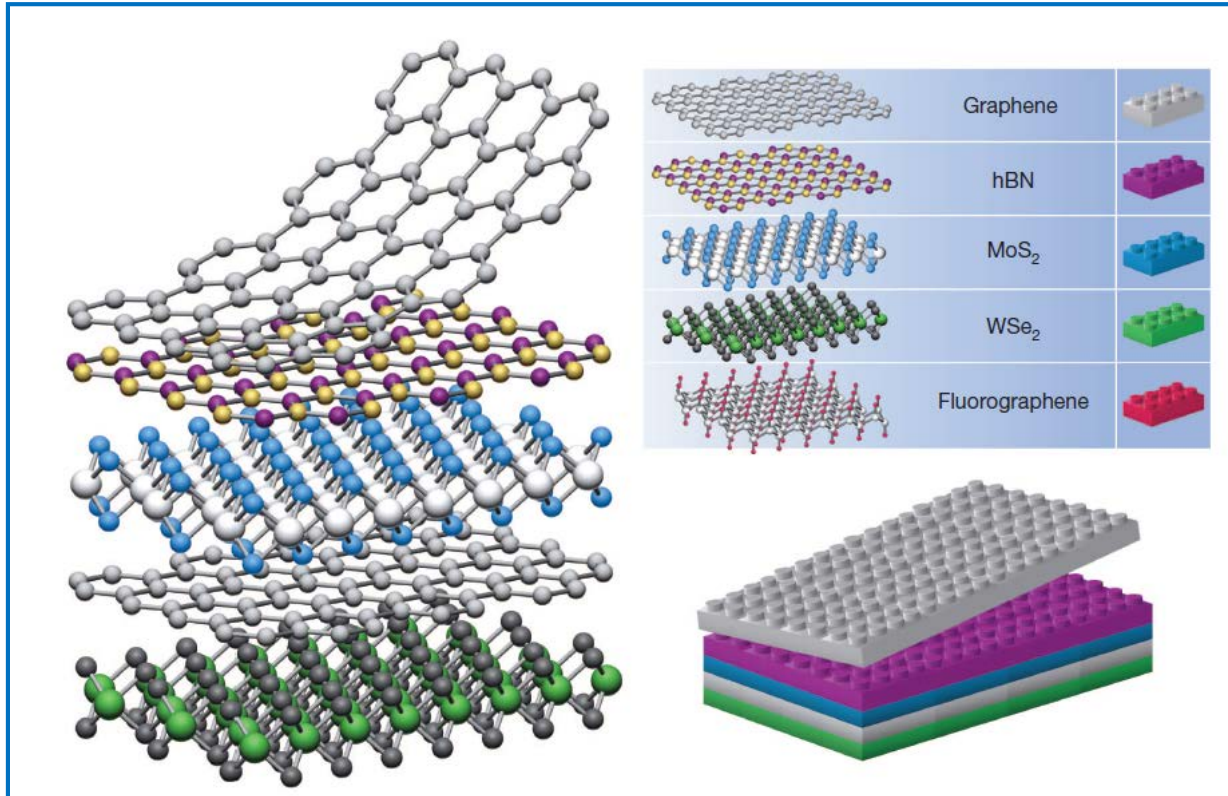
- The electronic structure associated with the MoS<sub>2</sub> shows obvious twist-angle dependence, specifically a VBM shift between  $\Gamma$  and K.

→ **twist-angle-dependent strain**

→ **charge redistribution at the interface**



# Van der Waals heterostructures



## Building van der Waals Heterostructures:

If one considers 2D crystals to be analogous to Lego blocks (right panel), the construction of a huge variety of layered structures becomes possible.

Conceptually, this atomic scale Lego resembles molecular beam epitaxy, but employs different 'construction' rules and a distinct set of materials.

# Current 2D library

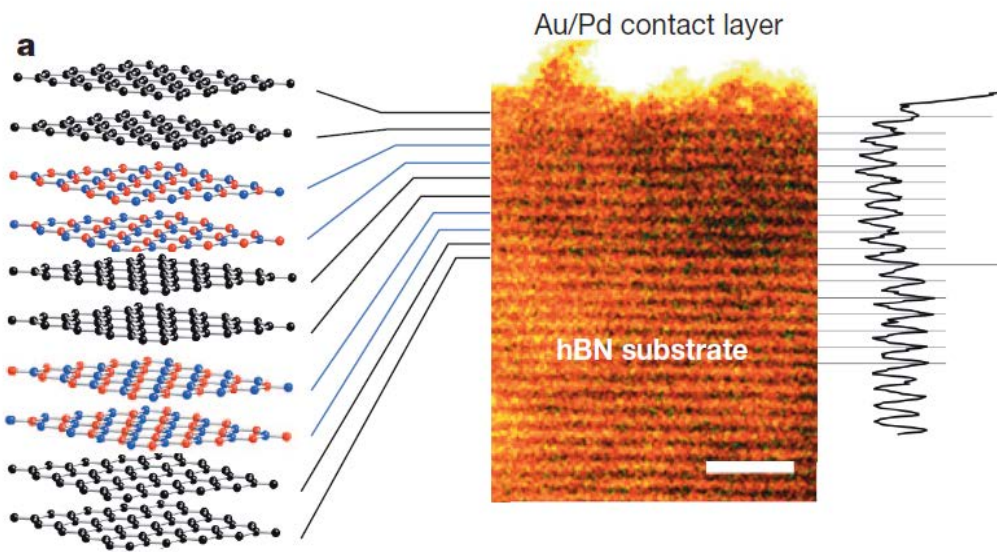
- Monolayers proved to be stable under room temperature in air are shaded **blue**;
- Those probably stable in air are shaded **green**;
- Those unstable in air but that may be stable in inert atmosphere are shaded **pink**.
- **Grey** shading indicates 3D compounds that have been successfully exfoliated down to monolayers.
- We note that, after intercalation and exfoliation, the oxides and hydroxides may exhibit stoichiometry different from their 3D parents.

| Graphene family  | Graphene  | hBN<br>'white graphene'   | BCN  | Fluorographene | Graphene oxide   |
|------------------|---|---|--|----------------|--|
| 2D chalcogenides | MoS <sub>2</sub> , WS <sub>2</sub> , MoSe <sub>2</sub> , WSe <sub>2</sub> | Semiconducting dichalcogenides:<br>MoTe <sub>2</sub> , WTe <sub>2</sub> ,<br>ZrS <sub>2</sub> , ZrSe <sub>2</sub> and so on | Metallic dichalcogenides:<br>NbSe <sub>2</sub> , NbS <sub>2</sub> , TaS <sub>2</sub> , TIS <sub>2</sub> , NiSe <sub>2</sub> and so on  |                |  |
|                  |   |   | Layered semiconductors:<br>GaSe, GaTe, InSe, Bi <sub>2</sub> Se <sub>3</sub> and so on   |                |  |
| 2D oxides        | Micas,<br>BSCCO   | MoO <sub>3</sub> , WO <sub>3</sub>  | Perovskite-type:<br>LaNb <sub>2</sub> O <sub>7</sub> , (Ca,Sr) <sub>2</sub> Nb <sub>3</sub> O <sub>10</sub> ,<br>Bi <sub>4</sub> Ti <sub>3</sub> O <sub>12</sub> , Ca <sub>2</sub> Ta <sub>2</sub> TiO <sub>10</sub> and so on |                | Hydroxides:<br>Ni(OH) <sub>2</sub> , Eu(OH) <sub>2</sub> and so on |
|                  | Layered<br>Cu oxides  | TiO <sub>2</sub> , MnO <sub>2</sub> , V <sub>2</sub> O <sub>5</sub> ,<br>TaO <sub>3</sub> , RuO <sub>2</sub> and so on      |  |                | Others   |

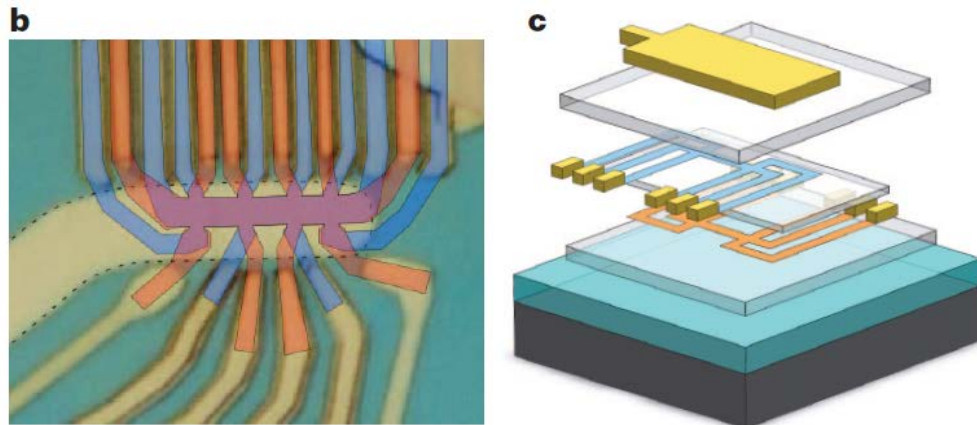
# *2-D Hetero-structures and applications*

- ❑ 2-D materials offer stacked like cards in a deck to create the different electronic layers as needed in functional electronic devices. **Van der Waals bonding**
- ❑ Because they do not form tight bonds with the layers above and below.
- ❑ Ye's group at Purdue reported to use both  $\text{MoS}_2$  and phosphorene to make ultrathin photovoltaics (PVs).
- ❑ Geim et al reported in Nature Materials to have assembled multiple 2D materials to make efficient thin LEDs.
- ❑ Revolution in electronics and optics just began.
- ❑ Flexible, transparent, temperature stable, and cheap to manufacture

## State-of-the-art van der Waals structures and devices

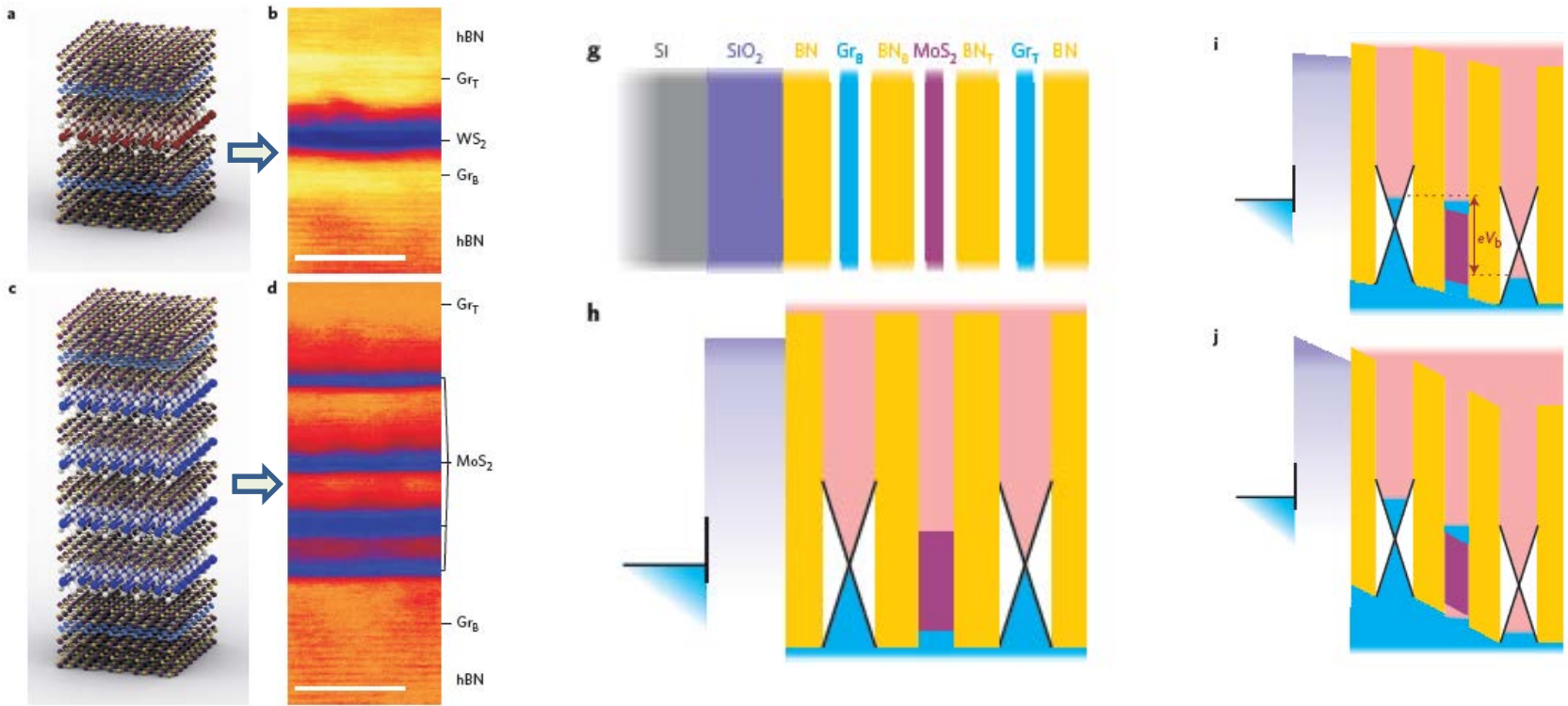


**a, Graphene–hBN superlattice** consisting of **six stacked bilayers**. On the right its cross-section and intensity profile as seen by scanning transmission electron microscopy are shown; on the left is a schematic view of the layer sequence. The topmost **hBN** bilayer is not visible, being merged with the metallic contact.



**b, c, Double-layer graphene heterostructures.** An optical image of a working device (b), and its schematics in matching colors (c). Two graphene Hall bars are accurately aligned, separated by a trilayer hBN crystal and encapsulated between relatively thick hBN crystals (hBN is shown in c as semitransparent slabs). The entire heterostructure is placed on top of an oxidized Si wafer (SiO<sub>2</sub> is in turquoise). **The colors in b indicate the top (blue) and bottom (orange) Hall bars and their overlapping region (violet).** The graphene areas are invisible in the final device image because of the top Au gate outlined by dashes. The scale is given by the width of the Hall bars, 1.5  $\mu\text{m}$ .

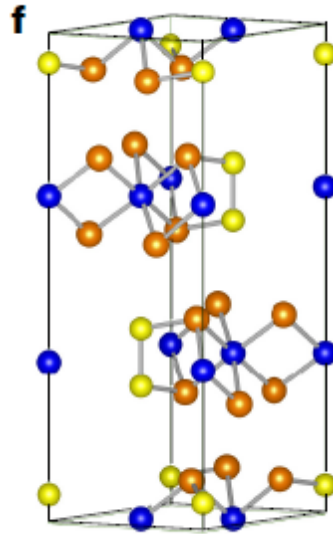
# Heterostructure devices with SQW and MQWs by band structure engineering



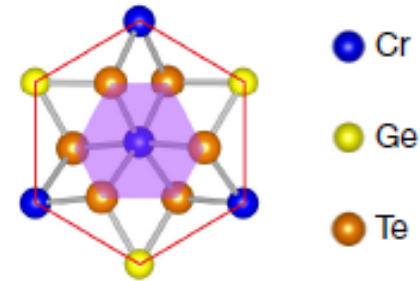
- a.** Schematic of the **SQW** heterostructure: hBN/Gr<sub>B</sub>/2hBN/WS<sub>2</sub>/2hBN/Gr<sub>T</sub>/hBN.
- b.** Cross-sectional bright-field STEM image of the type of heterostructure presented in a. Scale bar, 5 nm.
- c.d.** Schematic and STEM image of the **MQW** heterostructure: hBN/Gr<sub>B</sub>/2hBN/MoS<sub>2</sub>/2hBN/MoS<sub>2</sub>/2hBN/MoS<sub>2</sub>/2hBN/MoS<sub>2</sub>/2hBN/Gr<sub>T</sub>/hBN. The number of hBN layers between MoS<sub>2</sub> QWs in **d** varies. Scale bar, 5 nm.
- g.** Schematic of the heterostructure Si/SiO<sub>2</sub>/hBN/Gr<sub>B</sub>/3hBN/MoS<sub>2</sub>/3hBN/Gr<sub>T</sub>/hBN.
- h–j.** Band diagrams for **(h)** the case of zero applied bias; **(i)** intermediate applied bias; and **(j)** high bias for the heterostructure presented in **g**.

# Ferromagnetism in 2-D materials

- In 2-D systems, long-range magnetic order is strongly suppressed by thermal fluctuations, according to *the Mermin-Wagner theorem*.
- These thermal fluctuations can be counteracted by magnetic anisotropy.

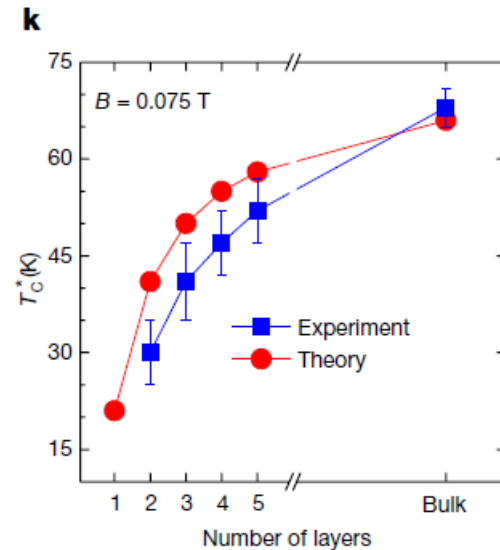
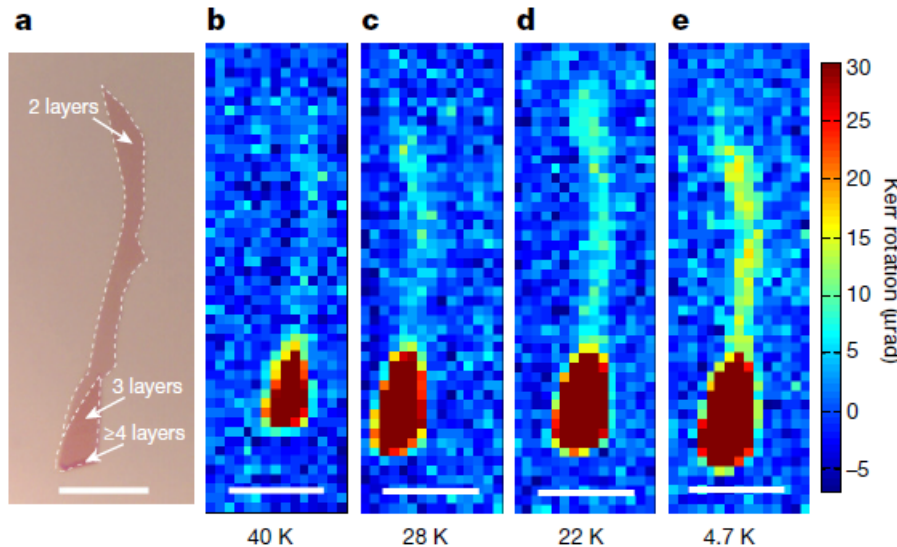


CrGeTe<sub>3</sub> with T<sub>c</sub> of 70K



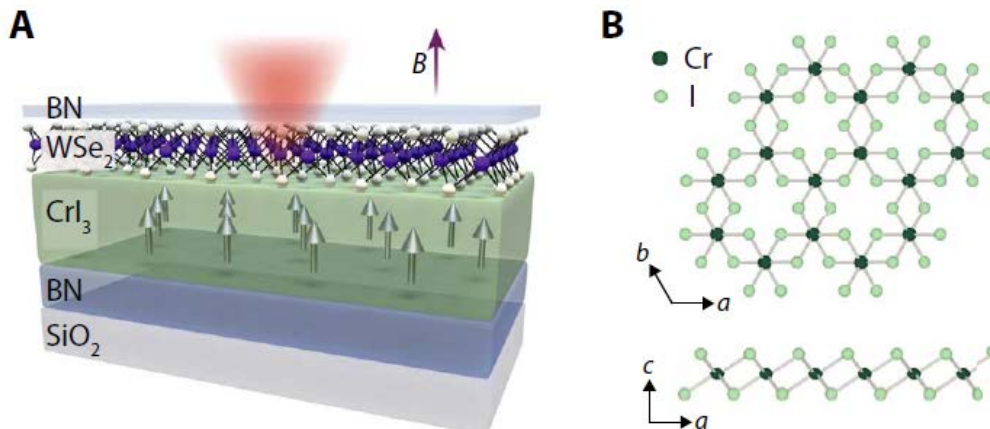
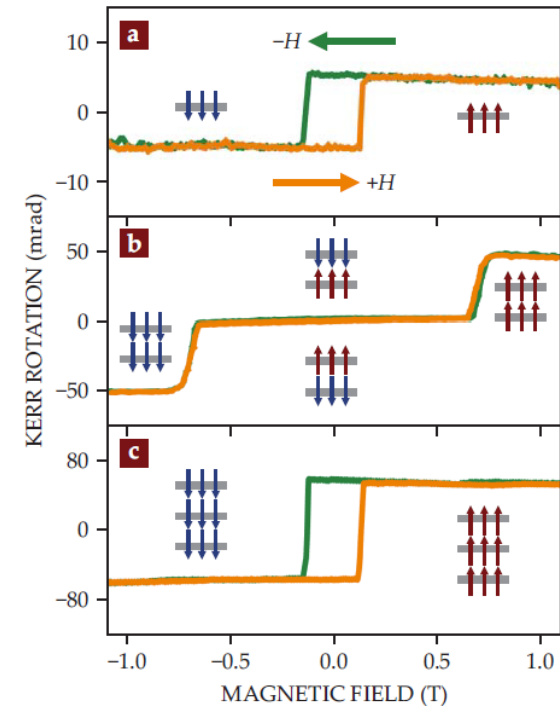
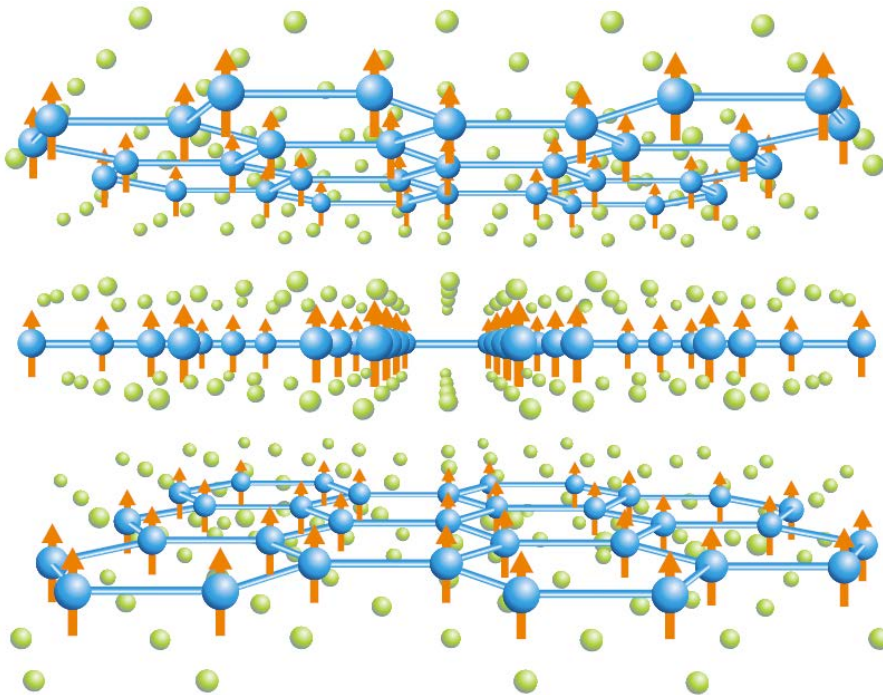
Xiang Zhang group of UC Berkeley

C. Gong et al., *Nature* **546**, 265 (2017).



# 2-D ferromagnet $\text{CrI}_3$ ( $T_c = 60\text{K}$ ) and the heterostructure

University of Washington's Xiaodong Xu  
& MIT's Pablo Jarillo-Herrero



B. Huang et al., *Nature* **546**, 270 (2017).

- Van der Waals heterostructures formed by an ultrathin ferromagnetic semiconductor  $\text{CrI}_3$  and a monolayer of  $\text{WSe}_2$
- Unprecedented control of the spin and valley pseudospin in  $\text{WSe}_2$